Data Folding for the LIGO Stochastic Directional Analysis Pipeline: Interim Report #2

Eli Wiston
University of Pennsylvania

Mentors: Arianna Renzini and Colm Talbot
California Institute of Technology
(Dated: August 19, 2021)

While a growing number of individual gravitational wave events have been observed, researchers are still searching for a stochastic gravitational-wave background. This superposition of weak, unresolved gravitational-wave signals could hold a wealth of both astrophysical and cosmological information. Studying both the isotropic and anisotropic components of the background at current detector sensitives could provide a measure of matter distributions and large-scale structure in the Universe. Eventually these searches may provide concrete evidence of inflation and act as a primordial analog to the Cosmic Microwave Background. This paper will detail the development of a data folding algorithm for the stochastic gravitational wave background analysis pipeline. Taking advantage of the fact that detector response is periodic with the rotation of the Earth, long stretches of time series data can be condensed to the size of one sidereal day. I implement this algorithm in both simulated and real data and verify it's efficacy through direct comparison to calculations with unfolded data. With the implementation of data folding, anisotropic directional searches can be carried out far more efficiently. Data folding only needs to be applied once, but brings orders of magnitude improvements in speed and data size, with negligible loss of information.

I. INTRODUCTION

In 2015, LIGO made the first direct detection of a gravitational wave (GW) signal. Since then, interferometers have measured many more signals from black hole and neutron star binaries. These binaries must either have very high mass or be very compact in order to be detected by current ground-based detectors. However, the sky is filled with gravitational wave signals below detection thresholds that, when analyzed as a whole, contain a great deal of information. These signals are unresolved, numerous, and best described according to probability distributions, hence they are known as the stochastic gravitational wave background (SGWB).

SGWB searches can be performed as either all-sky or directional searches. Isotropic searches model the background with no directional dependence and can be used to characterize the average GW signal in the universe. Directional searches account for potential variation across the sky and can be used to map anisotropies in the GW distribution. Due to the Earth's rotation, ground-based detectors measure a signal from each part of the sky over a sidereal day.

This project is focused on developing a key component of LIGO's SGWB pipeline: data folding. Because LIGO data is periodic over one day, we can compress the time series information we measure. By folding gravitational wave data over one sidereal day, we can vastly improve the efficiency of current and future directional stochastic searches.

The contents of this report will be presented as follows. In Section 2, I present a brief overview of the motivations for stochastic gravitational wave searches. In Section 3, I provide the necessary background, starting with gravitational waves in general and then going over stochastic signals and their measurement and analysis. Section 4 presents the goals and objectives of this specific project. Section 5 shows the data folding approach, modeled after the work in [1]. Section 6 details my progress in the first 7 weeks of the program. Finally, in Section 7, I describe the challenges and next steps for the project.

II. MOTIVATIONS

Gravitational waves allow researchers to probe the Universe without relying on electromagnetic signals. This can be incredibly useful, providing independent measurements of electromagnetic sources and new measurements of GW sources. High signal-to-noise measurements can provide insight into individual events, but the stochastic gravitational wave background can provide information about large scale structure and cosmology.

The earliest electromagnetic signals come from the time of last scattering, at a redshift of around $z = 1100$, and comprise the Cosmic Microwave Background (CMB) [2]. Before then, the universe was too opaque for photons to travel very far. However, gravitational waves were able to propagate all the way back in the early moments of the universe. Eventually, stochastic gravitational wave searches may be able to find direct evidence of inflation and provide information about early universe phase transitions.

Current detectors lack the sensitivity to measure the comparatively weak signals from these cosmological background events, but they can be used to study lower redshift astrophysical sources. These sources are expected to be distributed somewhat anisotropically. A direc-

tional search looking at these anisotropies in the SGWB can probe at the universe's underlying mass distribution. In particular, these searches can provide strong tests of the expected distribution of compact binary coalescences (CBCs)[3].

III. BACKGROUND

A. Gravitational Waves

Gravitational waves manifest as strains, or changes in length per unit length. They arise when the quadrapole mass moments of objects, I_{uv} have a time dependence [4]. This is why the direct detections already made involve compact mass objects inspiraling. In the context of general relativity, gravitational waves can be thought of as linear perturbations of the background metric g_{uv}. Assuming that the gravitational field is weak and non-stationary, one can show that the solution to the Einstein field equations for such a perturbation can be constructed as a plane wave, propagating at the speed of light [5].

Currently, the primary method for detecting gravitational waves is ground-based interferometry. The basic setup is that of a Michelson interferometer. A laser beam is split along two long, perpendicular arms and reflected off of mirrors, combining again at a photodetector. Gravitational waves strain the travel distance along the arms, creating an optical phase difference between the two beams. With a new phase difference, the electromagnetic laser waves interfere slightly differently, manifesting in a change in light intensity at the frequency of the wave, which one can directly measure. From these measurements, one may be able to determine the frequency, amplitude, direction, and polarization of the wave. Gravitational wave strains are incredibly small, so interferometers have to be extremely sensitive to detect them. There are many sources of noise that also make detection difficult, including seismic activity and Brownian motion of the detector mirrors [4].

B. Stochastic Signals

Due to the low signal-to-noise nature of gravitational waves, only the most extreme GW events can be directly detected. However, these types of events constitute a tiny fraction of all gravitational wave signals; the rest comprise the stochastic gravitational wave background. These stochastic signals are weak, independent, random, and unresolved. The distinction between a stochastic and resolvable signal can be unclear, as it may depend on modelling decisions or the precision of a detector. A signal can be operationally defined as stochastic if a Bayesian model selection calculation prefers a stochastic signal model over any deterministic signal model [2]. There are two broad categories of stochastic GW signals, based on the nature of the GW source: astrophysical and cosmological. Astrophysical signals occur at low redshift and are stochastic in the limit that number of sources N is very high. They are mainly comprised of compact binary systems. Cosmological signals arise from processes in the early Universe. They can be described stochastically as a result of the assumed homogeneity and isotropy of the universe. All inflationary models have some gravitational wave byproducts. Early universe phase transitions are also predicted to produce detectable signals [6]. LIGO does not currently have the sensitivity to measure weak cosmological signals, so this analysis will be aimed at measuring the astrophysical foreground.

A key parameter of interest in SGWB searches is Ω_{gw}, the fractional energy density of gravitational waves in the universe. The parameter can be expressed as $\Omega_{gw}(f, \hat{n})$, where f is the wave frequency and $\hat{n}$ is the direction [2]. Searches performed on LIGO's first three runs have not detected a stochastic background, but have set upper limits on Ω_{gw}. These limits fall in line with predictions based on the expected distribution of compact binary systems [3, 7].

C. Measurement and Analysis

The stochastic signal h_{ab} can be expressed as a superposition of sine waves as follows:

$$h_{ab}(t, \vec{x}) = \int_{-\infty}^{+\infty} df \int d^2\Omega_{\hat{n}} h_{ab}(t, \hat{n}) e^{i2\pi f(t+\hat{n}\cdot\vec{x}/c)} \quad (1)$$

where $h_{ab}(t, \hat{n})$ are the random variable Fourier coefficients that can be used to statistically describe the background. We can assume the background has zero mean, so $< h_{ab} >= 0$. For Gaussian sources, the signal is therefore entirely characterized by its second order moment. These quadratic expectation values can be defined in terms of the strain density power spectrum S_h. From S_h, $\Omega_{gw}(f)$ can be found through a simple relation:

$$S_h(f, \hat{n}) = \frac{3H_0^2}{8\pi^3} \frac{\Omega_{gw}(f, \hat{n})}{f^3} \quad (2)$$

The signal-to-noise of the stochastic background is far too low to extract any meaningful information from a single detector. However, by cross-correlating the strain data between multiple detectors, the stochastic signal can be found. The detectors will be measuring the same true signal, so those will add coherently. The noise in each detector, on the other hand, is independent and will not add coherently. Given a Gaussian approximation, the noise will be averaged down as $\frac{1}{\sqrt{time}}$, while the signal will be remain unsuppressed. The signal cross-correlation is directly related to key parameters, including S_h. By performing maximum likelihood analyses, one can calculate S_h from the observed cross-correlated data [2].

The longer the observation time being analyzed, the more the noise is suppressed. However, dealing with long periods of time is computationally demanding, both in

terms of processing power and storage. This issue can be confronted by folding the strain data. We fold over one sidereal day so anisotropies in the same region of the sky can add coherently. Ain, Dalvi, and Mitra developed the algebra and algorithm for such data folding [1]. Testing on LIGO S5 data, they found very significant decreases in computation time. An analysis of the full S5 data on folded data was faster than the same analysis of unfolded data by a factor of 300. Furthermore, the data quality was virtually unchanged; the differences between folded and unfolded maps were orders of magnitude smaller than the values themselves. The folding increases efficiency, portability, and convenience, facilitating more analyses of strain data, carried out at faster rates.

IV. OBJECTIVES

The goal of this project is to implement a data folding algorithm like [1] in Python for use in the LIGO stochastic gravitational wave pipeline. This folding should be performed as efficiently as possible, with negligible loss in data quality. By the end of the project, we hope to conduct a proof of principle test with mock data.

The data folding should be fixed to one sidereal day, as this will add anisotropic signals coherently for any Earth-based detector. However, the code should be flexible to allow for the addition of more detectors' data. At any given time, a detector is only sensitive to certain regions of the sky. The sensitivity of a set of detectors is given by the overlap function. As seen in FIG. 1 from [6], the overlap function for the two LIGO detectors has large areas of low sensitivity. While most of the sky will be covered as the Earth rotates, the sampling will be uneven. By designing our data folding code with the flexibility to allow the addition of more detectors, in new locations, we can enable a broader sampling of the sky.

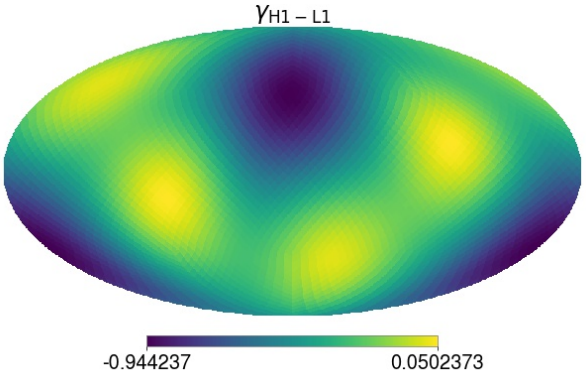

FIG. 1. Instantaneous overlap function for pairing of LIGO Hanford and LIGO Livingston detectors

V. APPROACH

The overall goal of a directional search is to estimate the amplitude of the SGWB power spectra density (PSD) as a function of position in the sky. For current searches, the shape of the PSD as a function of frequency is assumed. This assumption will work well for this project, since the PSD shape for the CBC dominated background is well known.

The time series data from a baseline of two detectors, $s(t)$ is the sum of the stochastic signal and detector noise. Following the approach in [1], it is convenient to divide the data for each baseline $\mathcal{I}$ into short time segments of length τ. A Fourier transform is then performed on each of these segments as follows:

$$\tilde{s}_{\mathcal{I}}(t;f) = \int_{t-\tau/2}^{t+\tau/2} dt' s(t') e^{-i2\pi f t'} \tag{3}$$

The maximum likelihood solution for the coefficients of the SGWB skymap, $\hat{P}$ can be calculated using two matrix quantities, the dirty map X and the Fisher information matrix Γ [2]:

$$\hat{P} = \Gamma^{-1} \cdot X \tag{4}$$

where,

$$X = \frac{4}{\tau} \sum_{Ift} \frac{H(f)\gamma^{I*}_{ft,\alpha}}{P_{I_1}(t;f)P_{I_2}(t;f)} \tilde{s}_{\mathcal{I}_1}(t;f)\tilde{s}^*_{\mathcal{I}_2}(t;f) \tag{5}$$

$$\Gamma = 4 \sum_{Ift} \frac{H^2(f)}{P_{I_1}(t;f)P_{I_2}(t;f)} \gamma^{I*}_{ft,\alpha}\gamma^{I}_{ft,\alpha'} \tag{6}$$

$H(f)$ is the expected shape of the stochastic background's frequency power spectral density. $P_{I_{1,2}}$ is the one-sided power spectral density of the noise for a segment of time. Since the noise dominates over the signal for short time segments, this quantity can be accurately estimated from the data. $\gamma^{I*}_{ft,\alpha}$ is the overlap function, containing all the specific information about the detectors' antenna pattern functions, baseline separations, and polarization basis.

Crucially, both quantities involve summations over all time segments. The time t can be re-expressed as $t = i_{day} \times T_s + t_s$, where i_{day} is the index of the sidereal day, T_s is the duration of a sidereal day, and t_s is the remaining time within a day. The summations over time can therefore be broken down into two parts $\sum_{i_{day}}$ and $\sum_{t_s}$. Performing the first sum folds the data, with the information from months or years compressed into one sidereal day. This process is shown below in FIG. 2, visualized by [1].

The data folding is somewhat complicated by the common application of window functions to the data. These functions help reduce spectral line leakage, but lead to an effective loss of data. To prevent this data loss, we

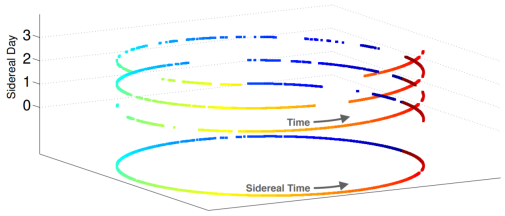

FIG. 2. Folding process visualized for 3 days of LIGO S5 data. The three top rings are projected onto the ring below, representing the folding data. Gaps in the rings represent missing data. [1]

use 50% overlapping windows in SGWB analysis. These overlaps lead to some additional complications in the data folding algebra, which manifest as corrections to the X and Γ, but do not impede our ability to fold the data [1].

VI. PROGRESS SO FAR

A. Working with Overlap Functions

As seen in the previous section, the overlap function γ is an essential quantity for SGWB calculations. γ describes the relationship between the power of the SGWB and the cross-correlated response of a baseline of two detectors [8]. Essentially, it is a measure of the baseline's sensitivity to different parts of the sky, which varies as a function of frequency and time.

To begin, I focused on visualizing these overlap functions as skymaps and seeing how they evolve in time. As seen in FIG. 3, the function has two large areas of maximum sensitivity and a band of minimum sensitivity separating them. Over the course of the day, the overlap function rotates along with the rotation of the Earth, completing one rotation each sidereal day. This periodicity is what allows my project to work. If the sensitivity is periodic over one sidereal day and the SGWB is relatively stationary, the response from each baseline should also be periodic each day. This is what enables us to fold a year's worth of data down to one day without loss of information.

Next, I looked at how these skymaps evolved with frequency. The frequency of the signal enters the overlap calculation through a factor of $e^{2\pi i f \Delta t}$, where Δt is the time delay between waves reaching both detectors. In FIG. 4, we see that as frequency increases, the overlap function develops more maxima and minima. With a higher frequency, there are more points where the signals arriving at each detector can go in and out of phase.

Alternatively, these skymaps can be visualized as "peanut plots," shown in FIG. 5. In these plots, the sky is represented 3-dimensionally. The radius of each point on the sphere represents the value of the overlap function

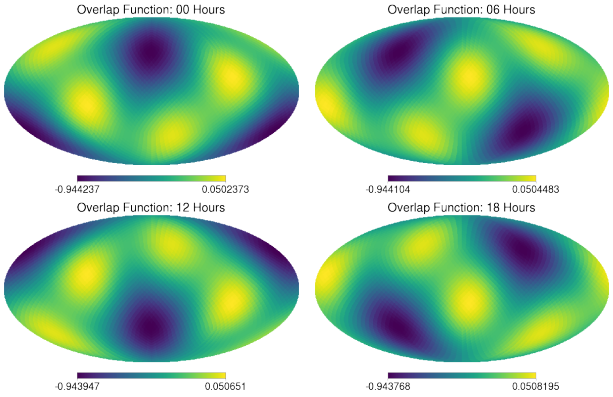

FIG. 3. The time-evolved overlap function for the baseline of the LIGO Hanford and LIGO Livingston detectors.

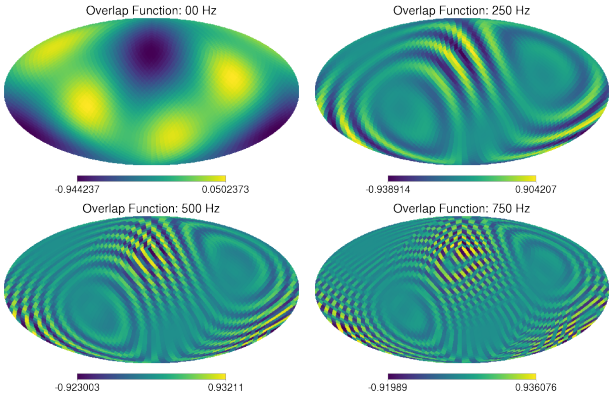

FIG. 4. The frequency-evolved overlap function for the baseline of the LIGO Hanford and LIGO Livingston detectors.

at that point. As these plots evolve in time, they spin in 3-dimensional space. As they evolve in frequency, the additional maxima and minima appear as spikes in the plot.

B. Spherical Harmonic Transformations

To gain further insight into these overlap functions, I worked on re-expressing them in terms of spherical harmonics. The spherical harmonic functions, Y^l_m, form a complete, orthonormal basis and, therefore, any function defined on the surface of a sphere can be re-written as a summation. For the overlap function:

$$\gamma(\theta,\phi) = \sum_{l,m} \gamma_{lm} Y^l_m(\theta,\phi) \tag{7}$$

The order of the harmonic l denotes the moment (monopole, dipole, etc.). The specific mode m corresponds to the frequency of oscillations. Each moment l has modes ranging from -l to +l. Each (l,m) mode can be found by integrating the overlap function multiplied

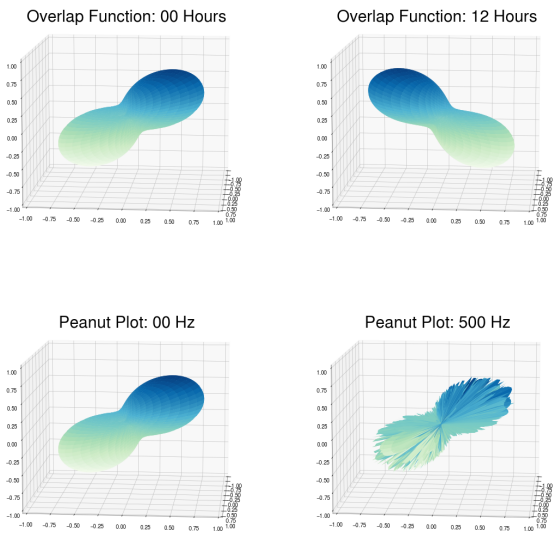

FIG. 5. Alternate visualization of how the overlap function evolves in frequency and time. The value of the function at any given point corresponds to the radius.

by the spherical harmonic over the sky.

$$\gamma_{lm} = \int d\Omega \gamma(\theta, \phi) Y^l_m(\theta, \phi) \tag{8}$$

In FIG. 6, this transformation is applied to the first 3 moments of the overlap function. As expected, the monopole term is constant in time. Due to the azimuthal symmetry of the system, all 3 dipole terms are equal to 0. The quadrupole terms illustrate how the mode number m corresponds to the frequency of oscillations. The $m = 0$ term is constant in time. The $m = -1, +1$ terms go through one period over the course of a day, while the $m = -2, +2$ terms go through two periods. A factor of $(-1)^m$ accounts for the reflection in the $-1, +1$ modes.

The power spectra for each moment can be calculated by summing over all the m modes in the following equation:

$$\Gamma_l = \frac{1}{2l+1} \sum_m |\gamma_{lm}|^2$$

The power for each moment at fixed time is shown in FIG. 7. Here we see that the azimuthal symmetry ensures that all odd moments drop to 0.

C. Correlating Simulated Data

Next, I started to work with the components of the dirty map and Fisher information matrix that will need to be folded: the power spectral densities (PSD) and the cross spectral density (CSD). The PSDs, or autocorrelations, are calculated by convolving the Fourier transformed data from a given detector with itself:

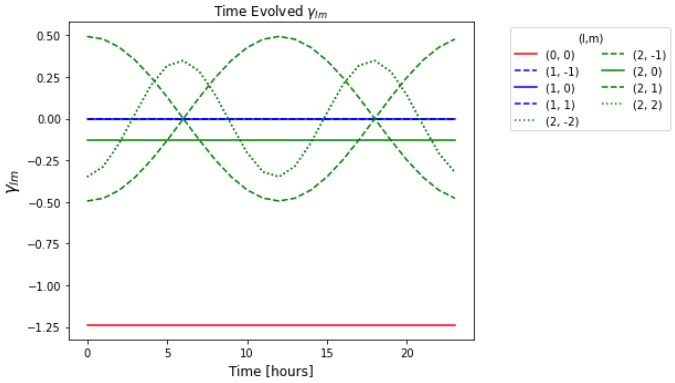

FIG. 6. First 3 γ_{lm} moments as a function of time. Monopole terms are shown in red, dipole in blue, and quadrupole in green.

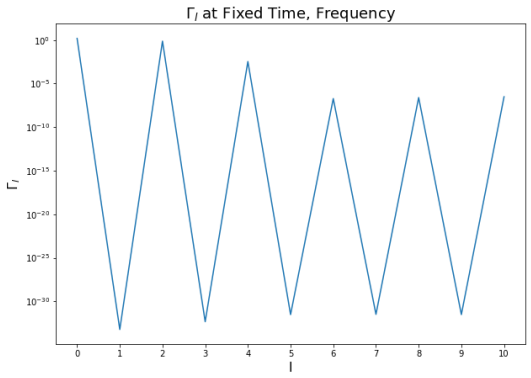

FIG. 7. Γ_l for the first 10 moments of the overlap function.

$$S_1 = \tilde{s}_{\mathcal{I}_1}(t; f)\tilde{s}^*_{\mathcal{I}_1}(t; f). \tag{9}$$

The CSD, or cross power, is calculated by convolving the data from two different detectors:

$$P_{12} = \tilde{s}_{\mathcal{I}_1}(t; f)\tilde{s}^*_{\mathcal{I}_2}(t; f). \tag{10}$$

Using the python package BILBY [9], I generated colored Gaussian time series data based on the LIGO design sensitivities for the Livingston and Hanford detectors. I then divided this time series into small time segments, performed Fast Fourier Transforms (FFT) on each segment, and averaged them together. This gave me the average Fourier transformed data needed to calculate autocorrelations and cross power. As expected, the autocorrelations resemble the design PSDs that originally colored the noise. The cross power maintains a similar shape, but the power has been averaged down. In order to see exactly how cross correlating has reduced the power, it is useful to look at a normalized quantity. The coherence term is equal to the CSD normalized by both

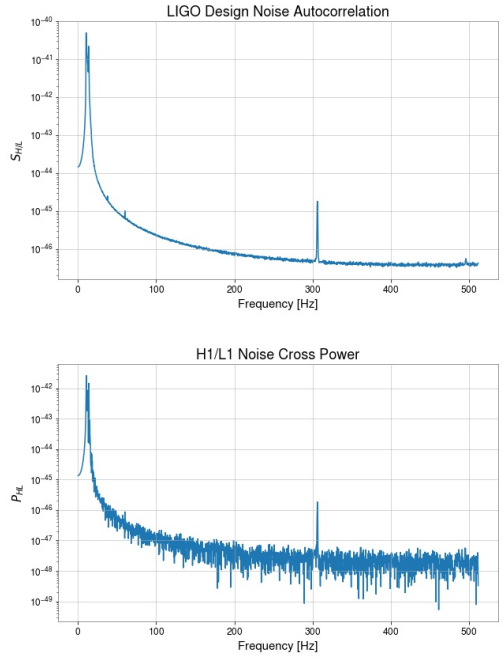

FIG. 8. Autocorrelation and cross power for simulated Hanford and Livingston colored Gaussian noise.

corresponding detector PSDs. For perfectly correlated data from two detectors at the same location, coherence is equal to 1. For the completely uncorrelated Gaussian noise from Bilby, the coherence is averaged down by $\frac{1}{\sqrt{N_{segments}}}$, where $N_{segments}$ is the number of short time segments being averaged over.

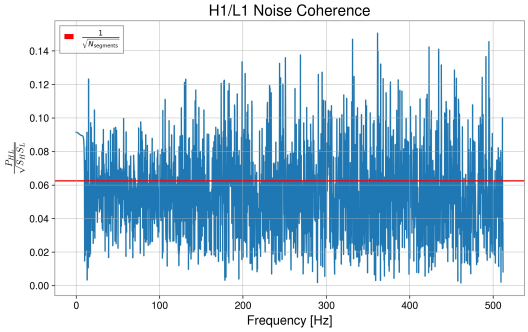

FIG. 9. Coherence for uncorrelated colored Gaussian noise from two LIGO detectors

Next, I injected a coherent signal into both detectors, centered at 200 Hz. The incoherent noise again averaged down by $\frac{1}{\sqrt{N_{segments}}}$, but the coherent signal remains at a coherence of 1. Here, we can see the value of looking at many days worth of data. The more days analyzed, the more time segments and the more the uncorrelated noise is suppressed relative to a coherent signal.

Instead of averaging over time segments, we can instead look at all time segments at once in a spectrogram. Looking at the time domain for our constant injected coherent signal isn't particularly illuminating. However, we can introduce some time dependence by modulating the coherent injection with a sinusoid of known period, mimic the modulation of a real GW detector response. In FIG. 11, we see this modulated injection, varying across time at 200 Hz.

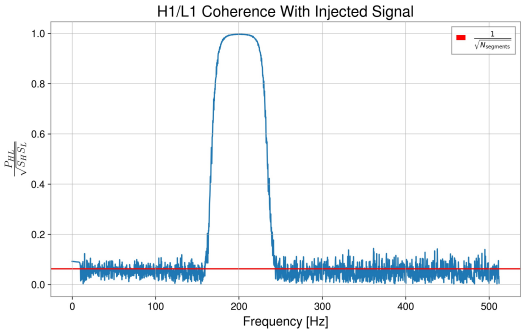

FIG. 10. Coherence for injected coherent signal in uncorrelated colored Gaussian noise from two LIGO detectors

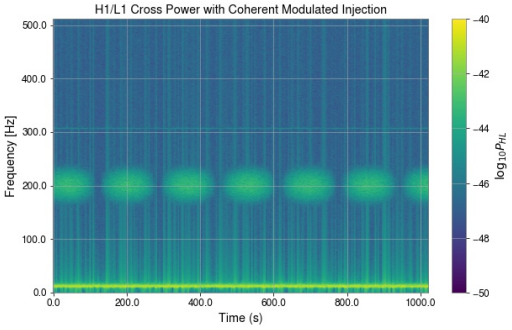

FIG. 11. Spectrogram view of an injected coherent signal modulated at fixed pweriod

D. Folding Simulated Data

The spectrogram in FIG. 11 acts like a very idealised stochastic signal. The period of oscillation is analogous to the stochastic response period of one sidereal day. Given that the signal is periodic and stationary, the spectrogram can be folded down to the size of one period (see FIG. 12).

Next, I worked with a week's worth of simulated stochastic data, provided by Liting Xiao. Like the previous spectrogram data, I was able to fold this cross power down to the size of one period, in this case the accurate value of one sidereal day (see FIG. 13). The simulated signal was a stochastic dipole, as may be observed in the two strong responses seen in one day.

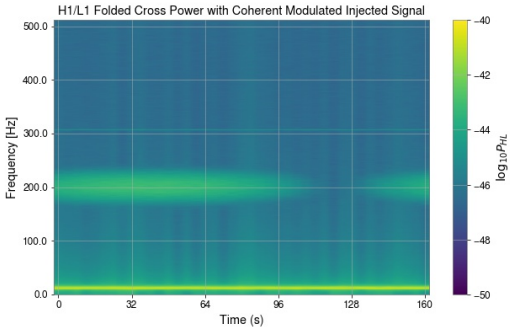

FIG. 12. Modulated injected signal folded over known period

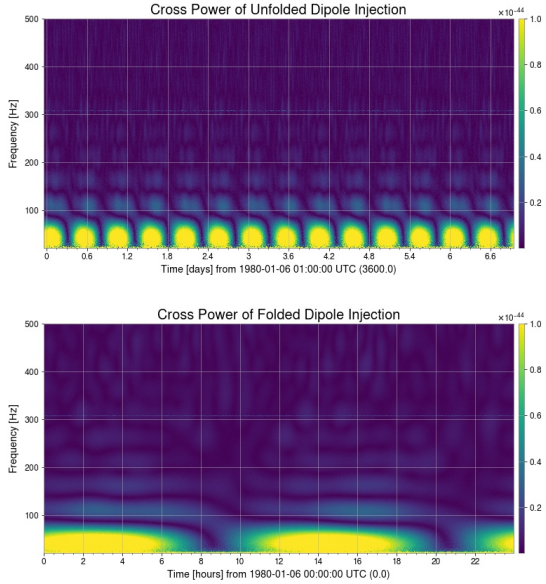

FIG. 13. Modulated injected signal folded over known period

E. Dirty Maps

As noted in the Approach section, the dirty map X is an important quantity for calculating the SGWB skymap. Noting that $H(f)$ is not time dependent and γ does not vary day to day, (5) can be broken into two summations:

$$X = \frac{4}{\tau} \sum_{I f t_s} H(f) \gamma^{I*}_{f t_s, \alpha} \sum_{i_{\rm day}} \frac{S_{12}(i_{\rm day} T_s + t_s; f)}{P_{1,2}(i_{\rm day} T_s + t_s; f)}, \quad (11)$$

where T_s is the length of a sidereal day and t_s is the time from the start of each day,

$$S_{12} = \tilde{s}_{\mathcal{I}_1}(i_{\rm day} T_s + t_s; f) \tilde{s}^*_{\mathcal{I}_2}(i_{\rm day} T_s + t_s; f), \quad (12)$$

and

$$P_{1,2} = P_{I_1}(i_{\rm day} T_s + t_s; f) P_{I_2}(i_{\rm day} T_s + t_s; f) \quad (13)$$

Performing the second summation folds the data down to the size of one sidereal day. This summation only needs to be performed once, but all subsequent analysis on folded data will be sped up by a factor of N_{days}.

Computing these dirty maps provides a useful way to determine whether data folding is working correctly. By computing maps using both (5) and (11), we can check to see if there are any significant differences, indicating a loss of information in the folding process. While the dirty map calculation involves a summation over frequencies, in order to save on computation time, it is sufficient to look at individual frequencies. At various frequencies, normalized difference maps were calculated as $\frac{|X_{\rm unfold} - X_{\rm fold}|}{\sqrt{X_{\rm unfold} X_{\rm fold}}}$ for the week of simulated dipole data (see FIG. 14).

At low frequency, the maps looked as expected, with the maximum difference between the unfolded and folded calculations being 0.2%. However, there were some complications at higher frequencies, with distinct spots of major differences of over 200%. This problem is currently being addressed, but it seems to be a numerical error linked to the oscillations of the overlap function at high frequency.

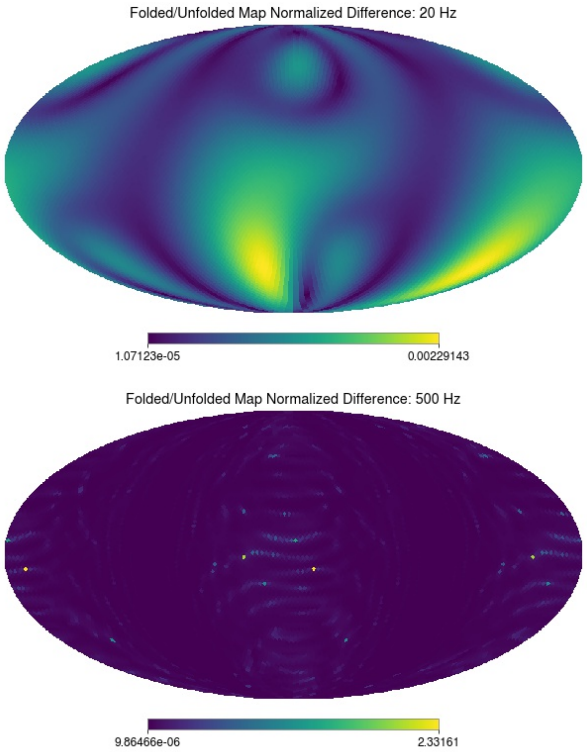

FIG. 14. Normalized difference between folded and unfolded dirty maps at 20 Hz and 500 Hz

F. Challenges

As seen in the previous section, I'm still working through some numerical issues with dirty maps at high frequency. Another significant challenge I've encountered

has to do with how to handle various time segment durations. Ideally, the segments would fit neatly into one sidereal day. However, a primary goal of this folding code is to allow for flexible use. Using any segment length that isn't a factor of one day inherently comes with a loss of information. There are two main methods to deal with this duration problem: cutting days down to be divisible by the given duration or lining times in each day up as close as possible, accepting that segments will be slightly offset from one another. From preliminary investigation, it seems that the latter option will result in less information loss, as seen in FIG. 15.

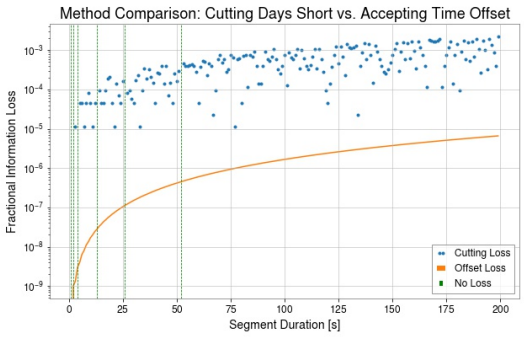

FIG. 15. Comparison of information loss between two methods of handling different segment durations. Across all reasonable segment choices, it appears accepting time offset will minimize information loss.

Moving forward, I anticipate a few issues to come up when I begin working with real data. The biggest challenge will likely be handling times where there are gaps in the data or data quality is poor. I will also have to line up the time series data from different detectors. Moving from a week's worth of data to a year may also come with challenges. I'll have to be more careful with how much memory is being used at a given time.

G. Next Steps

The next steps for my project will focus on the transition from simulated to real data. As mentioned in the previous section, I will have to add functionality to handle some of the complications that come with real data. Throughout implementation, I will also have to work to minimize information loss while still allowing for flexible use of the algorithm. For example, I will have to assess what the optimal methods are for handling different segment durations.

Another important step for the algorithm is applying corrections to the folding to account for windowing of the time segments. While this correction will be important future work, it will likely not fall within the timeline of this project.

[1] A. Ain, P. Dalvi, and S. Mitra, Fast gravitational wave radiometry using data folding, Phys. Rev. D **92**, 022003 (2015).

[2] J. Romano and N. Cornish, Detection methods for stochastic gravitational-wave backgrounds: A unified treatment, Living Reviews in Relativity **20** (2017).

[3] T. L. S. Collaboration, T. V. Collaboration, *et al.*, Upper limits on the isotropic gravitational-wave background from advanced ligo's and advanced virgo's third observing run (2021).

[4] H. Grote and D. H. Reitze, First-Generation Interferometric Gravitational-Wave Detectors, in *46th Rencontres de Moriond on Gravitational Waves and Experimental Gravity* (Moriond, Paris, France, 2011).

[5] B. F. Schutz, *A First Course in General Relativity* (Cambridge University Press, Cambridge, 2011).

[6] A. Renzini, *Mapping the gravitational-wave background*, Ph.D. thesis, Imperial College London (2020).

[7] B. Abbott *et al.* (The LIGO Scientific Collaboration and the Virgo Collaboration), Directional limits on persistent gravitational waves using data from advanced ligo's first two observing runs, Phys. Rev. D **100**, 062001 (2019).

[8] L. S. Finn, S. L. Larson, and J. D. Romano, Detecting a stochastic gravitational-wave background: The overlap reduction function, Phys. Rev. D **79**, 062003 (2009).

[9] G. Ashton, M. Hübner, P. D. Lasky, C. Talbot, K. Ackley, S. Biscoveanu, Q. Chu, A. Divakarla, P. J. Easter, B. Goncharov, and et al., Bilby: A user-friendly bayesian inference library for gravitational-wave astronomy, The Astrophysical Journal Supplement Series **241**, 27 (2019).